Journal of Catalysis 268 (2009) 142–149

Contents lists available at ScienceDirect

Journal of Catalysis

journal homepage: www.elsevier.com/locate/jcat

# La, V, and Fe promotion of $Rh/SiO_2$ for CO hydrogenation: Detailed analysis of kinetics and mechanism

Jia Gao, Xunhua Mo, James G. Goodwin Jr. *

*Department of Chemical and Biomolecular Engineering, Clemson University, Clemson, SC 29634, USA*

ARTICLE INFO

*Article history:*
Received 9 July 2009
Revised 3 September 2009
Accepted 12 September 2009
Available online 13 October 2009

*Keywords:*
Rh catalysts
La promotion
V promotion
Fe promotion
Mechanism
CO hydrogenation
Ethanol synthesis

ABSTRACT

It has been reported widely that Rh-based catalysts can exhibit high selectivity to $C_{2+}$ oxygenates during CO hydrogenation, with promoters playing an important role in this behavior. In this study, the effects of the addition of La, V, and/or Fe promoters on the kinetics of the formation of various products were determined and the mechanistic pathways were delineated using a Langmuir–Hinshelwood approach. Non-promoted and promoted Rh supported on $SiO_2$ were prepared using the incipient wetness impregnation method and were reduced in $H_2$ at 500 °C before reaction. The kinetic study was carried out using a fixed-bed differential reactor. It was found that, in general, increasing $H_2$ pressure resulted in increased activities, while increasing CO partial pressure had an opposite effect. However, the specific influence of $H_2$ or CO partial pressure on the activity and selectivities differed greatly with different promoters. There was a more significant change in the activity of the La–V doubly promoted Rh catalyst with $H_2$ or CO partial pressure than for other catalysts, which may be due to a synergistic effect between La and V. The Fe singly promoted catalyst showed different trends in both rate and selectivity from other catalysts, suggesting a different promoting mechanism than La or V. Based on the fact that hydrogen-assisted CO dissociation has been reported to best describe the mechanism for Rh catalysts, Langmuir–Hinshelwood rate expressions for the formation of methane and of ethanol were derived and compared to the experimentally derived power-law parameters. It was found that the addition of different promoters appeared to result in different rate-limiting steps.



## 1. Introduction

The hydrogenation of CO to form hydrocarbon and oxygenated products has been investigated by a host of researchers since the 1920s, but it was not until the 1980s that the ability of Rh-based catalysts to selectively produce $C_2$ oxygenates was pursued [1–4]. It has been suggested that the high performance of Rh-based catalysts for the formation of ethanol and other $C_{2+}$ oxygenates is due to the unique carbon monoxide adsorption behavior on Rh surfaces [1,2]. Since ethanol is a major fuel additive, a promising fuel alternative, and a means to store hydrogen in a liquid form for use in hydrogen fuel cells, Rh-catalyzed CO hydrogenation has attracted much attention in the last thirty years. Extensive research efforts have been devoted to study the influence of promoters on Rh-based catalyst characteristics and much detailed information can be found in several recent reviews [2–4].

In our previous studies [5–7], the effects of La, V, and Fe promotion of $Rh/SiO_2$ for CO hydrogenation have been investigated. It was found that the addition of La, V or Fe all increased the activity of $Rh/SiO_2$ to different extents, and the selectivites varied substantially with the addition of the different promoter(s). For instance, the addition of La resulted in a higher selectivity to ethanol, whereas the addition of V suppressed the formation of methane [6]. The addition of Fe, on the other hand, decreased the formation of higher hydrocarbons [7]. It was also determined that the combination of two or three different promoters resulted in significantly different catalytic activities. The La–V doubly promoted $Rh/SiO_2$ catalyst exhibited the highest activity and a moderate selectivity toward ethanol and other $C_{2+}$ oxygenates [5]. On the other hand, the La–V–Fe triply promoted $Rh/SiO_2$ catalyst showed the highest selectivity for ethanol for the reaction conditions utilized and a moderate activity [7]. It was also found that the addition of La enhanced CO chemisorption while V and Fe partially suppressed CO adsorption [7]. The addition of V or Fe also modified the $H_2$-TPD characteristics of $Rh/SiO_2$. It was proposed that the good performance of the multiply promoted catalyst was due to a synergistic promoting effect of the combined addition of different promoters through intimate contact with Rh.

The purpose of this study was to further probe the promoting mechanisms of these additives by investigating the effects of partial pressure of $H_2$ (in the range of 0.4–2.4 atm) and CO (in the range of 0.1–0.8 atm) on CO hydrogenation on the Rh-based catalysts. Moreover, the kinetic analysis was extended to determine

* Corresponding author. Fax: +1 864 656 078.
*E-mail address:* jgoodwi@clemson.edu (J.G. Goodwin).

0021-9517/$ - see front matter © 2009 Elsevier Inc. All rights reserved.
doi:10.1016/j.jcat.2009.09.012

the effects of different promoters on the mechanistic pathway for the formation of products. Methane formation was one focus for the mechanic pathway study in this investigation for the following reasons: (1) CO hydrogenation consists of a complex net of reaction pathways to form hydrocarbons and oxygenates. To derive a complete mechanism including the formation of every possible product is out of the scope of this study since our primary interest was to examine the promoting effect of different promoters. A study focused on $CH_4$, an important but undesirable product but with fewer required steps in the CO hydrogenation network, is more tractable. (2) Even though the CO hydrogenation network is complicated, it has been generally accepted that the first step in the synthesis of hydrocarbons and possibly $C_{2+}$ oxygenates is the formation of $CH_x$ ($x = 0–3$) species, which has also been suggested by many researchers to be the rate-limiting step on different catalysts [2,8–12]. Thus, a mechanistic study of $CH_4$ (formed by the hydrogenation of the $CH_x$ species) should shed some light on the effects of the promoters of interest on the formation of $C_{2+}$ oxygenates (formed mainly perhaps insertion of CO into a metal-$CH_x$ bond) and higher hydrocarbons (formed by mainly $CH_x$ chain growth). Because of the high value and versatile applications of ethanol compared to hydrocarbon products, the mechanism for the formation of ethanol was also studied in this research, which is likely somewhat related to that for the formation of methane.

## 2. Experimental

### 2.1. Catalyst preparation

Catalysts were prepared by sequential or co-impregnation as described in detail in our earlier study [5]. $Rh(NO_3)_3$ hydrate (Rh ~ 36 wt%, Fluka), $La(NO_3)_3{\cdot}6H_2O$ (99.99%, Aldrich) $NH_4VO_3$ (99.5%, Alfa Aesar), and $Fe(NO_3)_3{\cdot}9H_2O$ (98.0%, Alfa Aesar) were used as purchased. Silica gel (99.95%, Alfa Aesar) was first ground and sieved to 30–50 mesh, washed with boiled distilled water for 3 times, followed by calcination in air at 500 °C for 4 h before being used as a support (BET surface area after pretreatment was $250 \pm 2$ $m^2/g$). An aqueous solution of $Rh(NO_3)_3$ hydrate and/or precursors of the promoters (2 ml solution/1 g silica gel) was added dropwise to the silica gel until incipient wetness. The aqueous solution of $NH_4VO_3$ was prepared at elevated temperature (~80 °C) because of its low solubility at room temperature prior to mixing with other solutions; all the other aqueous solutions were prepared at room temperature. The catalyst precursor was dried at 90 °C for 4 h and then at 120 °C overnight before being calcined in air at 500 °C for 4 h.

### 2.2. Reaction

CO hydrogenation was conducted in a fixed-bed differential reactor (316 stainless steel) with length ~300 mm and internal diameter ~5 mm. A catalyst (0.3 g) and an inert ($\alpha$-$Al_2O_3$, 3 g) were loaded between quartz wool plugs, placed in the middle of the reactor with a thermocouple close to the catalyst bed. Ultrahigh-purity $H_2$ and CO (99.999%, National Welders) used in this work were purified by molecular sieve traps (Alltech) to remove $H_2O$, and CO was further purified using a CO purifier (Swagelok) to remove $CO_2$ and carbonyls. Prior to reaction, the catalyst was reduced in situ in hydrogen (flow rate = 30 mL/min, heating rate = 5 °C/min), holding at 500 °C for 1 h. The catalyst was then cooled down to the reaction temperature and the reaction started as gas flow was switched to $H_2$/CO ($H_2$ flow rate = 30 mL/min, CO flow rate = 15 mL/min) for the initial reaction study. Brooks 5840E series mass flow controllers were used to control flow rates. The kinetics study was carried out after the reaction reached steady state (in less than 15 h). In all cases, conversion was below 5% in order to assure differential conditions. Runs were repeated to determine repeatability and error (Tables 1 and 2). The apparent activation energies of CO conversion and different product formations were given by Arrhenius plots over the temperature range from 210 to 270 °C. In order to derive the apparent order of CO in the power rate law, $H_2$ partial pressure was kept at 1.2 atm ($H_2$ flow rate = 30 mL/min) and CO partial pressure varied from 0.1 to 0.8 atm. For example, for a CO partial pressure of 0.8 atm, the CO flow rate was set to 20 mL/min while $H_2$ flow rate was remained at 30 mL/min, and the total pressure was adjusted to 2.0 atm. For the apparent order of $H_2$, CO partial pressure was kept at 0.6 atm (CO flow rate = 15 mL/min) and $H_2$ partial pressure varied from 0.4 to 2.4 atm. We also carried out another series of experiments using He as a diluting agent for CO or $H_2$ to keep total pressure constant at 1.8 atm. The almost identical kinetic results (within 10% experimental error) obtained this way with what was obtained over a wider total pressure range indicated the validity of the kinetic study carried out by varying total pressure and the flow rate of one reactant but keeping the partial pressure and the flow rate of the other reactant constant. Due to the limitation of the experimental setup (e.g. the range of the CO MFC was smaller than that of the $H_2$ MFC), more reliable data points were able to be obtained by varying total pressure instead of using a diluting

**Table 1**
Composition and Catalytic activities of $SiO_2$-supported Rh-based catalysts.

| Nomenclature | Composition (wt%) and impregnation sequence[a] | Molar ratio of promoter/Rh | SS[f] Rate[b] (μmol/g/s) | Selectivity (%)[c] | | | | | |
|---|---|---|---|---|---|---|---|---|---|
| | | | | $CH_4$ | $C_{2+}$HC[d] | MeOH | Acetaldehyde | EtOH | Other $C_{2+}$ oxy[e] |
| Rh | Rh(1.5) | | 0.03 | 48.1 | 28.7 | 1.2 | 6.5 | 15.6 | – |
| RhLa | Rh(1.5)–La(2.6) | La/Rh = 1.3 | 0.07 | 38.8 | 27.4 | 4.1 | 8.3 | 21.5 | 0.1 |
| RhV | Rh(1.5)/V(1.5) | V/Rh = 2 | 0.09 | 12.6 | 64.1 | 6.0 | 1.5 | 13.6 | 1.5 |
| RhFe | Rh(1.5)–Fe(0.8) | Fe/Rh = 1 | 0.11 | 55.3 | 13.7 | 9.5 | 2.2 | 19.4 | – |
| RhLaV | Rh(1.5)– La(2.6)/V(1.5) | La/Rh = 1.3 V/Rh = 2 | 0.23 | 15.8 | 51.2 | 2.7 | 6.1 | 22.3 | 1.8 |
| RhLaFeV | Rh(1.5)–Fe(0.8)–La(2.6)/V(1.5) | La/Rh = 1.33 V/Rh = 2 Fe/Rh = 1 | 0.21 | 19.4 | 33.6 | 5.6 | 3.5 | 34.4 | 3.5 |

[a] For the catalysts referred to as Rh/M (M = La , V, or Fe promoter), silica gel was first impregnated with the aqueous solution containing the precursor of M and then impregnated by $Rh(NO_3)_3$ aqueous solution and calcination at 500 °C for 4 h. On the other hand, Rh–M refers to a catalyst prepared by co-impregnation. Numbers in parentheses following the symbol for an element indicate the weight percent of that element based on the weight of the silica gel support.
[b] Catalyst: 0.3 g; inert: α-alumina 3 g; pretreatment 500 °C; reaction conditions: $T = 230$ °C, $P = 1.8$ atm, flow rate = 45 mL/min ($H_2$/CO = 2), data taken at 15 h after steady state was reached; experimental error: ±5%.
[c] Molar selectivity = $n_iC_i / \sum n_iC_i$.
[d] Hydrocarbons with 2 or more carbons.
[e] Other oxygenates besides acetaldehyde and ethanol with 2 or more carbons.
[f] Steady state. SS rate = μmol CO conversed/gcat. s.

**Table 2**
Reaction orders[a,b,c,d] for the synthesis of $CH_4$, $C_2H_n$, $C_3H_n$, EtOH, and total CO conversion at 230 °C.

| Catalysts | CO conversion | | $CH_4$ formation | | $C_2H_n$ formation | | $C_3H_n$ formation | | EtOH formation | |
|---|---|---|---|---|---|---|---|---|---|---|
| | *x* | *y* | *x* | *y* | *x* | *y* | *x* | *y* | *x* | *y* |
| Rh | 0.55 | −0.26 | 1.03 | −0.67 | 0.61 | −0.35 | 0.07 | 0.11 | 1.02 | −0.13 |
| RhLa | 0.65 | −0.49 | 0.97 | −0.79 | 0.47 | −0.41 | 0.15 | −0.22 | 0.93 | −0.54 |
| RhFe | 0.58 | 0.03 | 0.69 | −0.11 | 0.11 | 0.35 | −0.14 | 0.53 | 0.51 | 0.30 |
| RhV | 0.84 | −0.31 | 1.35 | −0.71 | 0.88 | −0.41 | 0.61 | −0.26 | 1.09 | −0.22 |
| RhLaV | 0.88 | −0.65 | 1.37 | −0.74 | 0.8 | −0.4 | 0.65 | −0.32 | 1.17 | −0.45 |
| RhLaFeV | 0.75 | −0.21 | 1.10 | −0.55 | 0.49 | −0.25 | 0.32 | −0.16 | 0.94 | −0.16 |

[a] Catalyst: 0.3 g; inert: α-alumina 3 g; pretreatment: 500 °C in $H_2$; data taken at 15 h TOS after steady state was reached.
[b] The rate parameters for each catalyst are determined by fitting a power-law rate expression of the form $r = Ae^{-E_a/RT}P_{H_2}^{x}P_{CO}^{y}$.
[c] Error = ±10% for all the values measured.
[d] To determine *x*, $P_{CO}$ = 0.6 atm was used and $P_{H2}$ was varied from 0.4 to 2.4 atm; to determine *y*, $P_{H2}$ = 1.2 atm was used and $P_{CO}$ was varied from 0.46 to 0.8 atm.

agent, results reported in this paper were based on the data obtained by varying total pressure. The reaction rate did not change by varying space velocities or particle sizes, suggesting no existence of external and internal mass transfer, respectively. The activation energies of CO hydrogenation from Arrhenius plots was found to be ca. 25 kcal/mol, the expected value, and confirmed the absence of heat or mass transport limitations on the rate of reaction measurements.

The products, including hydrocarbons and oxygenates, were analyzed on-line by an FID (flame ionization detector) in a gas chromatograph (Varian 3380 series) with a Restek RT-QPLOT column. CO and other inorganic gases were analyzed by a TCD (thermal conductivity detector) after separation with a Restek HayeSep® Q column. The analysis details can be found in our previous paper [5]. The selectivity of a particular product was calculated based on carbon efficiency using the formula $n_iC_i/\sum n_iC_i$, where $n_i$ and $C_i$ are the carbon number and molar concentration of the *i*th product, respectively.

## 3. Results

### 3.1. Catalytic activities of Rh-based catalysts for CO hydrogenation

Table 1 shows preparation sequence, composition, and atomic ratio of promoter/Rh, steady-state rate, and selectivities for the different products of the catalysts at 230 °C and a flow rate of 45 mL/min ($H_2$/CO = 2), which are consistent with our previous studies [5–7]. All the reaction rates and selectivities were calculated without including $CO_2$ since negligible amounts below GC detection of $CO_2$ were formed for all the catalysts under the reaction conditions used in this study. Addition of the promoters modified both rate and selectivities. All La, V, and Fe enhanced activity and La and Fe boosted ethanol selectivity, while V suppressed methane selectivity. The La and V doubly promoted catalyst showed the highest activity. The triply promoted catalyst RhLaFeV was the best catalyst for ethanol (EtOH) formation at these reaction conditions because of the high activity and ethanol selectivity.

### 3.2. Influence of the partial pressure

The variations in steady-state reaction rate selectivities to $CH_4$, $C_2H_n$, $C_3H_n$, and EtOH obtained using the Rh-based catalysts at different $H_2$ or CO partial pressures are shown in Figs. 1 and 2. Methanol and acetaldehyde are not included here because the selectivities were too low to study the trends.

As presented in Fig. 1a, when $H_2$ partial pressure was increased from 0.4 to 2.4 atm with the partial pressure of CO held at 0.6 atm, the steady-state rate rose steadily for all the catalysts. The CO conversion rate on the doubly promoted RhLaV catalyst increased nearly 5 times, more significantly than all the other catalysts. However, with the addition of Fe as the third promoter, this increase was somewhat lower. In Fig. 1b, compared to the nonpromoted catalyst Rh for which the selectivity for $CH_4$ increased significantly with $H_2$ partial pressure; the addition of any of the promoters caused a lower increase. It is obvious that V-containing catalysts exhibit lower $CH_4$ selectivity compared to other catalysts even at higher $H_2$ partial pressure. The catalysts with by far the lowest $CH_4$ selectivities were RhV < RhLaV < RhLaFeV. Both $C_2H_n$ and $C_3H_n$ selectivities decreased with increasing $H_2$ partial pressure, with the promoters significantly affecting the absolute $C_2H_n$ and $C_3H_n$ selectivities as shown in Fig. 1c and d. As shown in Fig. 1e, the selectivity for EtOH increased somewhat with increasing $H_2$ partial pressure, except for the Fe singly promoted catalyst. For that catalyst, EtOH selectivity actually decreased a little with increasing $H_2$ partial pressure.

Fig. 2 presents the steady-state rate and selectivities for $CH_4$, $C_2H_n$, $C_3H_n$, and EtOH with the CO partial pressure varying from 0.1 to 0.8 atm and $H_2$ partial pressure held at 1.2 atm. In Fig. 2a, it can be seen that the total CO conversion rate was only slightly affected by increasing CO partial pressure for all the catalysts except for the La–V doubly promoted catalyst. The selectivity to $CH_4$ decreased with CO partial pressure for all the catalysts, as shown in Fig. 2b. Different from the effect of $P_{H2}$, the CO partial pressure did not affect $C_2H_n$ selectivities for any significant degree as shown in Fig. 2c. In Fig. 2d, it can be seen that, while the $C_3H_n$ selectivity for the nonpromoted Rh catalyst significantly increased with increasing CO partial pressure, those for all the promoted catalysts did not. The selectivity for EtOH increased somewhat with increasing CO partial pressure for the nonpromoted, Fe, and LaFeV promoted catalysts as shown in Fig. 2e. The other catalysts showed only small increases.

### 3.3. Power-law expression

The power-law rate parameters in the form of $r = Ae^{-E_a/RT}P_{H_2}^{x}P_{CO}^{y}$ for the synthesis of $CH_4$, $C_2H_n$, $C_3H_n$, EtOH, and total CO conversion are summarized in Tables 2 and 3. Since the formations of different products from CO hydrogenation follow somewhat different pathways, it is more meaningful to examine the power-law rate parameters for individual product rather than the rate parameters for the overall reaction of CO. The low standard deviations for the activation energy and reaction order measurements along with their correlation coefficients (>0.97) indicate that these parameters represent the data well. Results in the literature for kinetic parameters of CO hydrogenation on Rh catalysts vary significantly due to differences in pressure, temperature, and conversion [10,13,14].

As can be seen in Table 2, the *x* and *y* values varied for the different promoters, with all the results between −0.2 and 1.4 for the reaction order of $H_2$ and between −0.8 and 0.6 for that of CO. Our

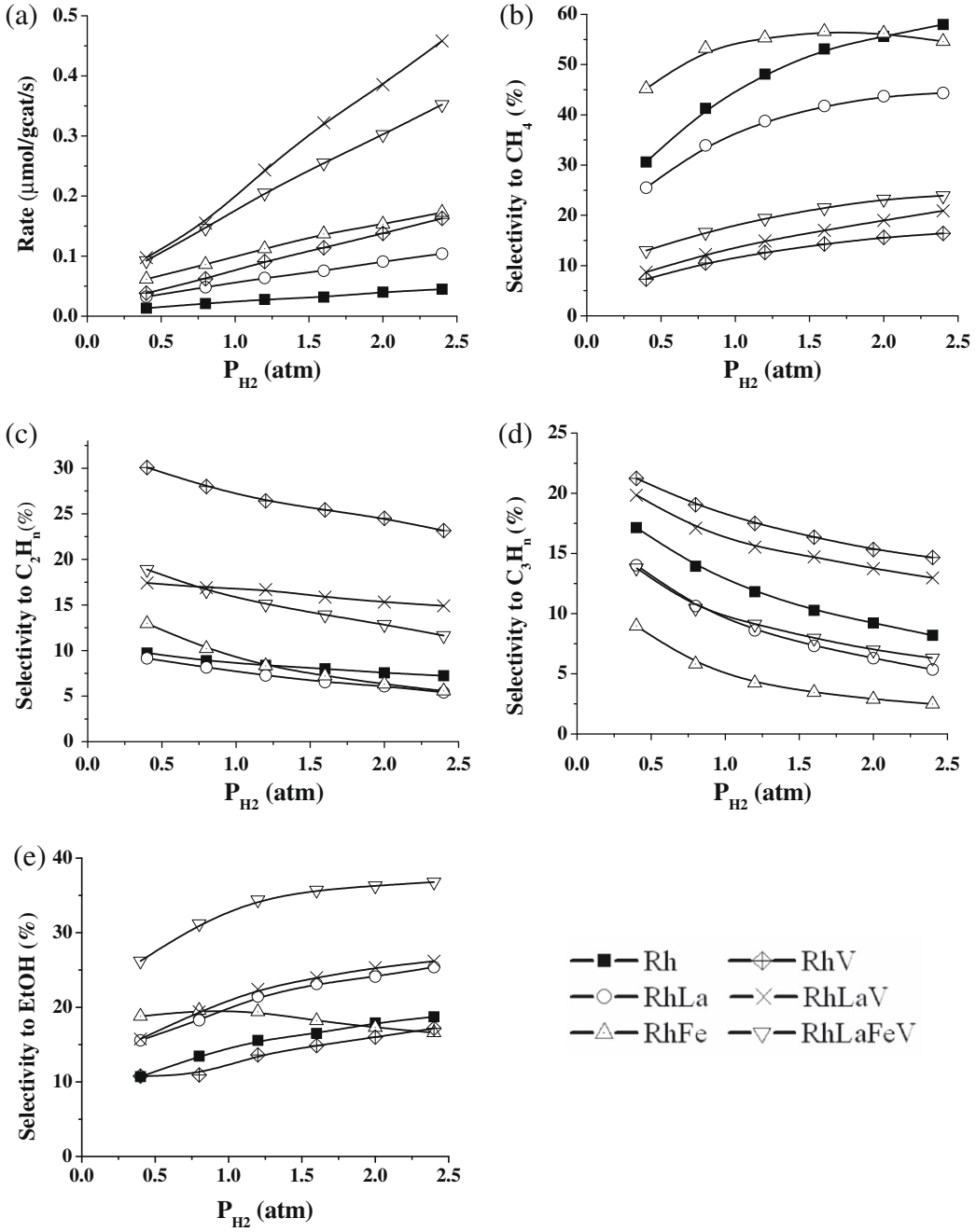


**Fig. 1.** The effect of $H_2$ partial pressure on (a) CO conversion rate, (b) selectivity to $CH_4$, (c) selectivity to $C_2H_n$, (d) selectivity to $C_3H_n$, and (e) selectivity to EtOH at 230 °C.

results in Table 3 for activation energies are consistent with the published data [13,14]. It can be seen that, in general, the activation energies were higher for the La-promoted catalysts but lower for the Fe-promoted ones compared to the nonpromoted catalyst. Thus, based on the results shown in Tables 2 and 3, it is quite obvious that the effects of the addition of different promoters were quite different.

## 4. Discussion

### 4.1. Effects of promoters on kinetics

It is widely accepted that $H_2$ and CO adsorption on a catalyst surface are two key factors in the CO hydrogenation process. In Fig. 1b–d, the selectivity for $CH_4$ increases slightly and the selectivities for higher hydrocarbons decrease with increasing $H_2$ partial pressure. This is understandable because the increased hydrogen coverage on a Rh-based catalyst surface would definitely increase the hydrogenation of $CH_x$ species, leading to more methane. On the other hand, increased $H_2$ partial pressure may also decrease CO adsorption and dissociation, resulting in less chain growth. It can be seen in Fig. 1e that EtOH showed a different trend from $C_2H_n$ or $C_3H_n$ on all the catalysts, indicating that the formation of ethanol involves a different pathway compared to the formation of higher hydrocarbons. On a catalyst surface, an increase in CO adsorption may result in a decrease in $H_2$ adsorption, as a result of which $CH_4$ selectivity would decrease. Thus, as seen in Fig. 2b, increasing CO partial pressure resulted in a decrease in $CH_4$ selectivity for all catalysts. There was also an increase in EtOH selectivity for all the catalysts (Fig. 2e).

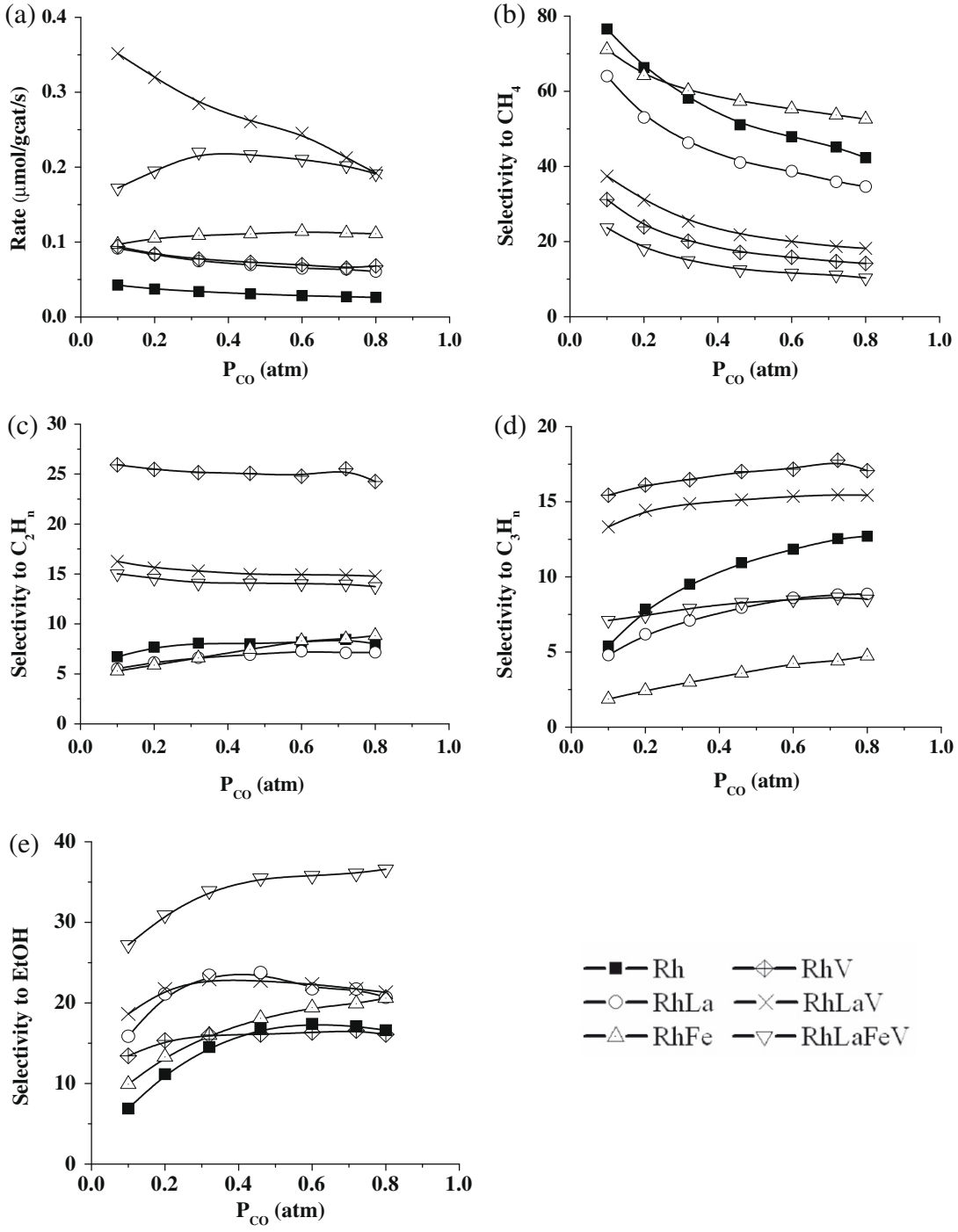


**Fig. 2.** The effect of CO partial pressure on (a) CO conversion rate, (b) selectivity to $CH_4$, (c) selectivity to $C_2H_n$, (d) selectivity to $C_3H_n$, and (e) selectivity to EtOH at 230 °C.

As evidenced by IR, chemisorption, and CO-TPD [7,15–18], CO adsorption is enhanced by La addition, especially when small amounts of La are added. As a result, adding La increases the activity compared to nonpromoted $Rh/SiO_2$ as seen in Figs. 1a and 2a. In Table 2, the reaction orders of CO for the La-promoted catalysts were more negative compared to those for the nonpromoted catalyst, almost certainly due to the promotion of CO adsorption by La addition as found in our previous work [5], leading to a greater decrease in reaction rate with increasing partial pressure of CO. However, judging from the fact that the hydrogen reaction orders for all the products on RhLa did not change much compared to those for Rh, the main function of the addition of La appears not to be an enhancement of hydrogenation as suggested by Borer and Prins [18]. In what seems contradictory, La addition increases the activity of $Rh/SiO_2$ by increasing CO adsorption but this also causes the rate to have a higher negative order in CO partial pressure.

Addition of V also increased the activity as shown in Figs. 1a and 2a. This is understandable because, even though CO adsorption is partially suppressed by V addition [5], the activity of adsorbed CO may actually increase at the catalytic surface [6]. There are also some interesting differences in the orders of reaction between RhLa and RhV. Contrary to the case for RhLa, hydrogen reaction orders for all species on RhV were larger than those on Rh while that for CO was almost the same, showing higher dependency on

**Table 3**
Activation energy[a,b,c,d] for the synthesis of $CH_4$, $C_2H_n$, $C_3H_n$, EtOH, and total CO conversion.

| Catalysts | CO conversion | $CH_4$ formation | $C_2H_n$ formation | $C_3H_n$ formation | EtOH formation |
|---|---|---|---|---|---|
| Rh | 25.6 | 29.2 | 29.6 | 24.3 | 18.3 |
| RhLa | 27.4 | 31.6 | 30.2 | 30 | 24.2 |
| RhFe | 21.5 | 23.9 | 22.6 | 23 | 15.7 |
| RhV | 26.9 | 30.9 | 28.5 | 28.5 | 17.6 |
| RhLaV | 27.4 | 30.5 | 28.4 | 29.5 | 21.3 |
| RhLaFeV | 25.3 | 28.2 | 27.6 | 27.4 | 21.5 |

[a] Catalyst: 0.3 g; Inert: α-alumina 3 g; Pretreatment: 500 °C in $H_2$; Data taken at 15 h TOS after steady state was reached.
[b] At constant flow rate = 45 mL/min ($H_2$/CO = 2), $P$ = 1.8 atm, the activation energy for each catalyst is determined by $\ln r = \ln A - \frac{E_a}{RT}$ while temperature varied from 210 to 270 °C.
[c] Error = ±10% for all the values measured.
[d] The unit of activation energy is kcal/mol.

hydrogen. This result is consistent with the TPD results from our previous study, which showed a reduced $H_2$ desorption around the reaction temperature with the addition of V [7]. Several research groups have proposed that the addition of V boosts hydrogenation [19–22]. The seeming discrepancy between these results and the ones here may be due to one or more of the following reasons: (1) the conditions for catalyst preparation and pretreatment are different, and it is well known that these conditions strongly affect the interactions between V and Rh [23–25] leading to a different catalytic behavior; (2) even if V boosts $H_2$ desorption at a higher temperature as claimed by some researchers [19], it is questionable whether these strongly bonded H atoms would be available for the reaction under normal reaction conditions.

The activity of RhLaFeV did not change as much as RhLaV with $H_2$ partial pressure in Fig. 1a. The sharper decrease in $C_2H_n$ selectivity with increasing $H_2$ partial pressure observed on Fe-promoted catalysts in Fig. 1c may be due to an improved hydrogenation ability which leads to more methanol and methane. Burch and Petch [26] have suggested that Fe may act as a reservoir for spillover $H_2$ on the surface of Rh catalysts. Also, since the presence of Fe increases the availability of hydrogen (or the efficiency with which hydrogen is utilized) and at the same time suppresses CO adsorption [7], the dependence on CO partial pressure for RhFe is different from that for RhLa or RhV as shown in Fig. 2a and in Table 2. In addition, the enhanced hydrogen adsorption could interfere with CO adsorption, which might account for the hindering effect on EtOH selectivity with increasing $H_2$ partial pressure for RhFe, as shown in Fig. 1e.

### 4.2. Mechanistic study

#### 4.2.1. Methane formation

The mechanism for the formation of methane will now be addressed, which may shed some light on how the different promoters affect CO hydrogenation. However, even for methane formation, there are disagreements in the literature about whether C–O bond cleavage occurs in CO hydrogenation via direct dissociation (carbide models [8,9,11,27–31]) or via a hydrogen-assisted process [10,12,32–43]. There has been an increasing focus more recently on the hydrogen-assisted mechanism because several authors have provided strong evidence supporting this mechanism, especially for Rh-based catalysts [10,32–39,41–43]. Based on isotopic analysis comparing hydrogen to deuterium, Mori et al. [41,43] suggested that the rate-limiting step for CO hydrogenation is the dissociation of $H_nCO$, where $n$ = 1, 2 or 3. Based on BOC-MP calculations, Shustorovich and Bell [42] supported the hypothesis that the dissociation of $H_nCO$ is more favorable than the direct dissociation of CO on Pd and Pt. Later, Bell and co-workers suggested that both CO and $CO_2$ hydrogenation go through hydrogen-assisted dissociation to form methane on Rh [10,39].

By comparing various proposed mechanism with the power-law parameters in Table 2, most could be ruled out with the exception of that of Bell and co-workers. Because of its similarity that mechanism but with more detail regarding hydrogen-assisted CO dissociation for gas methane formation, the model of Holmen and co-workers [34] was chosen to describe the mechanism for CO hydrogenation under our reaction conditions, even though it was originally written for CO hydrogenation on Co. As shown in Fig. 3, the sequence begins with the adsorption of CO and dissociation of $H_2$. Then the adsorbed CO is hydrogenated to produce $CH_xO$ species, which subsequently dissociate to form adsorbed $CH_3$ and O species.

In order to determine the rate-limiting steps for the methane formation for our promoted Rh catalysts, a Langmuir–Hinshelwood approach was used with the mechanism given in Fig. 3 to derive rate expressions for different possible rate-limiting steps, which can be compared with power-law parameters to verify the mechanism and to better understand the effects of the promoters on the reaction. In Fig. 3, Steps (7), (8), and (9) are believed to reach equilibrium too quickly to be considered as rate-limiting steps [34]. Since adsorbed CO occupies most of the surface sites on Rh [44,45] and CO conversion is very low (<5%), the intermediates to produce other products should not occupy a significant part of the active sites and therefore are left out of the adsorption term (the denominator) of the derived rate expressions.

The rate expressions derived assuming one of the steps from Steps (1)–(6) in Fig. 3 as the rate-limiting step are shown in Table 4, where $k_i$ is the kinetic parameter. $K_i$ is an equilibrium constant for the $i$th step in Fig. 3. The concentration of vacant active sites [S] is determined from a balance of the total concentration of the active sites [$S_0$] which is assumed to be constant. [$S_0$] is equal to

$$\frac{1}{2}H_2 + S \longleftrightarrow H - S \quad (1)$$

$$CO + S \longleftrightarrow CO - S \quad (2)$$

$$CO - S + H - S \longleftrightarrow CHO - S + S \quad (3)$$

$$CHO - S + H - S \longleftrightarrow CH_2O - S + S \quad (4)$$

$$CH_2O - S + H - S \longleftrightarrow CH_3O - S + S \quad (5)$$

$$CH_3O - S + S \longleftrightarrow CH_3 - S + O - S \quad (6)$$

$$O - S + H - S \longleftrightarrow HO - S + S \quad (7)$$

$$HO - S + H - S \longleftrightarrow H_2O + 2S \quad (8)$$

$$CH_3 - S + H - S \longleftrightarrow CH_4 + 2S \quad (9)$$

**Fig. 3.** Proposed mechanism for $CH_4$ formation.

**Table 4**
Rate-limiting step assumed and the resulted rate expression in various possibilities for $CH_4$ formation.

| Possible rate-limiting step for $CH_4$ from Fig. 3 | Rate expressions | $x$[a] | $y$[a] |
|---|---|---|---|
| 1 | $\frac{k_1[S_0]P_{H_2}^{1/2}}{[1+K_2P_{CO}]}$ | 0.5 | $-1 < y < 0$ |
| 2 | $\frac{k_2[S_0]P_{CO}}{[1+K_1(P_{H_2})^{1/2}]}$ | $-0.5 < x < 0$ | 1 |
| 3 | $\frac{k_3K_2K_1[S_0]^2P_{H_2}^{1/2}P_{CO}}{[1+K_1(P_{H_2})^{1/2}+K_2P_{CO}]^2}$ | $-0.5 < x < 0.5$ | $-1 < y < 1$ |
| 4 | $\frac{k_4K_3K_2K_1^2[S_0]^2P_{H_2}P_{CO}}{[1+K_1(P_{H_2})^{1/2}+K_2P_{CO}+K_3K_2K_1P_{H_2}^{1/2}P_{CO}]^2}$ | $0 < x < 1$ | $-1 < y < 1$ |
| 5 | $\frac{k_5K_4K_3K_2K_1^3[S_0]^2P_{H_2}^{3/2}P_{CO}}{[1+K_1(P_{H_2})^{1/2}+K_2P_{CO}+K_3K_2K_1P_{H_2}^{1/2}P_{CO}+K_4K_3K_2K_1^2P_{H_2}P_{CO}]^2}$ | $0.5 < x < 1.5$ | $-1 < y < 1$ |
| 6 | $\frac{k_6K_5K_4K_3K_2K_1^3[S_0]^2P_{H_2}^{3/2}P_{CO}}{\left[1+K_1(P_{H_2})^{1/2}+K_2P_{CO}+K_3K_2K_1P_{H_2}^{1/2}P_{CO}+K_4K_3K_2K_1^2P_{H_2}P_{CO}+K_5K_4K_3K_2K_1^3P_{H_2}^{3/2}P_{CO}\right]^2}$ | $-1.5 < x < 1.5$ | $-1 < y < 1$ |

[a] $x$, $y$ would be the orders of reaction of $H_2$ and CO in the equivalent power-law rate expression $r = Ae^{-E_a/RT}P_{H_2}^{x}P_{CO}^{y}$.

[S] plus the sum of all sites occupied by reactants and products. In Table 4, the ranges of possible reaction orders $x$ and $y$ in an equivalent power-law rate expression based on the derived mechanistic rate expression are given assuming that step to be rate limiting. Comparing the ranges of the possible reaction orders with the experimental power-law results for $CH_4$ formation in Table 2, Step 1, 2 or 3 as the rate-limiting step cannot fit the experimental data because all the apparent orders for $H_2$ for the different catalysts were larger than 0.5. For Rh and RhLa, the apparent order for $H_2$ partial pressure was approximately equal to 1 (Table 2). It is generally agreed that the $H_2$ desorption activation energy is relatively low and most of the active sites are occupied by CO on Rh and RhLa [9,27,33–35]. Thus, the $H_2$ terms in the denominator are reported to be statistically insignificant and can be neglected in the mechanistic rate expression. As a result, Step (4) (resulting $H_2$ exponent ~1) is more likely to be the rate-limiting step than either Step (5) or (6) (resulting $H_2$ exponent ~1.5).

For the Fe singly promoted $Rh/SiO_2$ catalyst, it is to be expected that $x$ (0.7 as shown in Table 2) is a little bit different from the La promoted or nonpromoted catalysts because the concentration of hydrogen on the surface should no longer be ignored since the addition of Fe leads to a significant suppression of CO adsorption, although CO adsorption still occupies most of the active sites on surface as a result of weakening $H_2$ adsorption as determined by Egawa et al. using HREELS and TPD methods [46]. Since Steps (1), (2), and (3) have already been ruled out for all the catalysts, the rate-limiting step should be Step (4), (5) or (6). Also, it is not practical to compare these three possibilities as for RhLa or Rh because $H_2$ terms in the denominator can no longer be ignored compared to CO terms.

The $H_2$ power-law parameters for $CH_4$ formation are larger than 1.0 for RhV (1.35) and RhLaV (1.37), thus, the rate-limiting step for these two catalysts may be either Step (5) or (6). This is suggested by other data since the V addition hinders CO adsorption but increases desorption/reactivity of adsorbed CO species [6], which, thus, may result in a change in the rate-limiting step. However, for RhLaFeV, step 4 could also be the rate-limiting step even though $x = 1.1$ and is only slightly >1. Thus, $x = 1.1$ can be considered to be within experimental and Langmuir–Hinshelwood error of $x = 1.0$.

It is difficult to distinguish different possible rate expressions or figure out the values of the equilibrium constants by our present work due to the complexity of the mechanism and the assumptions required using the Langmuir–Hinshelwood approach. Nevertheless, a sound conclusion can be drawn here is that the addition of different promoters resulted in different rate-limiting steps, which can be ascribed to the modified $CO/H_2$ adsorption, reactivity of adsorbed species on $Rh/SiO_2$ promoted by different promoters.

#### 4.2.2. Ethanol formation

Since ethanol synthesis is one of the key issues of CO hydrogenation, extensive efforts have been focused on the mechanism of ethanol formation. However, since the insertion step may occur through different reaction routes-insertion of $CH_xO$ into a metal-$CH_x$ bond ($x$ = 0, 1, 2 or 3), there are few detailed results in the literature regarding the ethanol synthesis mechanism on Rh. A scheme, however, is proposed in Fig. 4 based on methane formation mechanism. Moreover, this mechanism of ethanol formation is similar to the mechanism Holmen and co-workers [34] proposed for Co catalysts by comparing the activation energies for possible insertion steps by microkinetic modeling.

In Table 2, it can be seen that the even though the reaction order for $H_2$ partial pressure did not change much between methane and ethanol formation, the reaction order for CO partial pressure chan-

$$\frac{1}{2}H_2 + S \longleftrightarrow H-S \quad (1)$$

$$CO + S \longleftrightarrow CO-S \quad (2)$$

$$CO-S + H-S \longleftrightarrow CHO-S+S \quad (3)$$

$$CHO-S+H-S \longleftrightarrow CH_2O-S+S \quad (4)$$

$$CH_2O-S+H-S \longleftrightarrow CH_3O-S+S \quad (5)$$

$$CH_3O-S+S \longleftrightarrow CH_3-S+O-S \quad (6)$$

$$O-S+H-S \longleftrightarrow HO-S+S \quad (7)$$

$$HO-S+H-S \longleftrightarrow H_2O+2S \quad (8)$$

$$CH_3-S+CH_2O-S \longleftrightarrow CH_3CH_2O-S+S \quad (9`)$$

$$CH_3CH_2O-S+H-S \longleftrightarrow CH_3CH_2OH+2S \quad (10`)$$

**Fig. 4.** Proposed mechanism for EtOH formation.

**Table 5**
Rate-limiting step assumed and the resulted rate expression in various possibilities for EtOH formation.

| Possible rate-limiting step for EtOH from Fig. 4 | Rate expression | $x$[a] | $y$[a] |
|---|---|---|---|
| 9′ | $\frac{k_{10}K_9K_8K_6K_5K_4^2K_3^2K_2^2K_1^7[S_0]^2P_{H_2O}^{-1}P_{H_2}^{7/2}P_{CO}^2}{\left[1+K_1(P_{H_2})^{1/2}+K_2P_{CO}+K_3K_2K_1P_{H_2}^{1/2}P_{CO}+K_4K_3K_2K_1^2P_{H_2}P_{CO}+K_5K_4K_3K_2K_1^3P_{H_2}^{3/2}P_{CO}+K_9K_8K_6K_5K_4K_3K_2K_1^5P_{H_2}^{5/2}P_{CO}P_{H_2O}\right]^2}$ | $-1.5 < x < 3.5$ | $0 < y < 2$ |
| 10′ | $\frac{k_{11}K_{10}K_9K_8K_6K_5K_4^2K_3^2K_2^2K_1^8[S_0]^2P_{H_2O}^{-1}P_{H_2}^{4}P_{CO}^2}{\left[1+K_1(P_{H_2})^{1/2}+K_2P_{CO}+K_3K_2K_1P_{H_2}^{1/2}P_{CO}+K_4K_3K_2K_1^2P_{H_2}P_{CO}+K_5K_4K_3K_2K_1^3P_{H_2}^{3/2}P_{CO}+K_9K_8K_6K_5K_4K_3K_2K_1^5P_{H_2}^{5/2}P_{CO}P_{H_2O}+K_{10}K_9K_8K_6K_5K_4^2K_3^2K_2^2K_1^7[S_0]^2P_{H_2O}^{-1}P_{H_2}^{7/2}P_{CO}^2\right]^2}$ | $-3 < x < 4$ | $-2 < y < 2$ |

[a] $x$, $y$ would be the orders of reaction of $H_2$ and CO in the equivalent power-law rate expression $r- = Ae^{-E_a/RT}P_{H_2}^xP_{CO}^y$.

ged significantly. Thus, it can be concluded that there are different rate-limiting steps for ethanol and methane formation: (1) since the rate expressions for the rate-limiting step of steps (1)–(6) were already evaluated in determining the rate-limiting step for methane formation and (2) since the rate-limiting step for ethanol and methane appears to be different, it is unlikely that the adsorption of CO or $H_2$ (step (1) and (2)) or the synthesis of $CH_3$ species (step (3)–(6)) provides the rate-limiting step for ethanol. Thus, most likely, the rate-limiting step for ethanol formation is step (9′) or (10′); steps (7) and (8) being earlier ruled out as they were fast. Table 5 shows these two possibilities and the ranges of apparent reaction orders $x$ and $y$ based on the derived Langmuir–Hinshelwood mechanistic rate expressions. Since most of the reaction orders for CO partial pressure are negative in Table 2, the rate-limiting step in ethanol formation mechanism should be Step (10′) for all the catalysts except perhaps RhFe. However, it is difficult to distinguish between Step (9′) and (10′) for RhFe because the reaction order for CO partial pressure on RhFe is higher than for others (around 0.30).

## 5. Conclusions

A series of Rh-based catalysts with single or combined promoters among La, V, and Fe were prepared by sequential or co-impregnation method. A kinetics study of CO hydrogenation on these catalysts was conducted to understand the mechanism and the role of promoters.

All the catalysts except RhFe and RhLaFeV showed the same trends in CO conversion and selectivities to different products with increasing CO or $H_2$ partial pressure. The influence of partial pressure to activity is more obvious for RhLaV than for other catalysts, which appears due to a synergistic promoting effect of La and V. For the Fe-promoted catalysts, the CO conversion rate increases with CO partial pressure, which may be because Fe serves like a reservoir to hydrogen on the catalyst surface.

The parameters obtained from power law were used to fit the rate expressions derived based on different limiting steps to understand the reaction mechanism and the effects of different promoters. The fact that coefficient $x$ is positive and the coefficient $y$ is negative indicates promotion by hydrogen and inhibition by carbon monoxide. By comparing the power-law parameters with the Langmuir–Hinshelwood rate expression, $CHO - S + H - S \leftrightarrow CH_2O + S$ is more likely to be the rate-limiting step for the methane formation on Rh and RhLa. The rate-limiting step for the methane formation on RhV and RhLaV is $CH_2O - S + H - S \leftrightarrow CH_3O - S + S$ or $CH_3O - S + S \leftrightarrow CH_3 - S + O - S$. For ethanol synthesis, $C_2H_5O - S + H - S \leftrightarrow C_2H_5OH + 2S$ is the possible rate-limiting step for all the catalysts except for RhFe. However, it is unclear that whether $CH_3 - S + CH_2O - S \leftrightarrow C_2H_5O - S + S$ or $C_2H_5O - S + H - S \leftrightarrow C_2H_5OH + 2S$ is the rate-limiting step for ethanol synthesis on RhFe.

## Acknowledgment

We acknowledge financial support from the U.S. Department of Energy (Award No. 68 DE-PS26-06NT42801).

## References

[1] J.P. Hindermann, G.J. Hutchings, A. Kiennemann, Catal. Rev.-Sci. Eng. 35 (1993) 1.
[2] S.S.C. Chuang, R.W. Stevens Jr., R. Khatri, Top. Catal. 32 (2005) 225.
[3] J.J. Spivey, A. Egbebi, Chem. Soc. Rev. 36 (2007) 1514.
[4] V. Subramani, S.K. Gangwal, Energy Fuels 22 (2008) 814.
[5] J. Gao, X. Mo, A.C. Chien, W. Torres, J.G. Goodwin Jr., J. Catal. 262 (2009) 119.
[6] X. Mo, J. Gao, J.G. Goodwin Jr., Catal. Today 147 (2009) 139.
[7] X. Mo, J. Gao, N. Umnajkaseam, J.G. Goodwin Jr., J. Catal. (2009), in press, doi:10.1016/j.jcat.2009.08.007.
[8] B. Sarup, B.W. Wojciechowski, Can. J. Chem. Eng. 67 (1989) 620.
[9] B. Sarup, B.W. Wojciechowski, Can. J. Chem. Eng. 67 (1989) 62.
[10] I.A. Fisher, A.T. Bell, J. Catal. 162 (1996) 54.
[11] J.M.H. Lo, T. Ziegler, J. Phys. Chem. C 111 (2007) 11012.
[12] O.R. Inderwildi, S.J. Jenkins, D.A. King, J. Phys. Chem. C 112 (2008) 1305.
[13] R.P. Underwood, A.T. Bell, Appl. Catal. 21 (1986) 157.
[14] P. Gronchi, S. Marengo, C. Mazzocchia, E. Tempesti, R. DelRosso, React. Kinet. Catal. Lett. 60 (1997) 79.
[15] R.P. Underwood, A.T. Bell, J. Catal. 111 (1988) 325.
[16] R.P. Underwood, A.T. Bell, J. Catal. 109 (1988) 61.
[17] A.L. Borer, R. Prins, Stud. Surf. Sci. Catal. 75 (1993) 765.
[18] A.L. Borer, R. Prins, J. Catal. 144 (1993) 439.
[19] H.Y. Luo, H.W. Zhou, L.W. Lin, D.B. Liang, C. Li, D. Fu, Q. Xin, J. Catal. 145 (1994) 232.
[20] T. Koerts, R.A. Vansanten, J. Catal. 134 (1992) 13.
[21] T. Beutel, O.S. Alekseev, Y.A. Ryndin, V.A. Likholobov, H. Knoezinger, J. Catal. 169 (1997) 132.
[22] H.Y. Luo, W. Zhang, H.W. Zhou, S.Y. Huang, P.Z. Lin, Y.J. Ding, L.W. Lin, Appl. Catal. A: Gen. 214 (2001) 161.
[23] S. Ishiguro, S. Ito, K. Kunimori, Catal. Today 45 (1998) 197.
[24] T. Beutel, V. Siborov, B. Tesche, H. Knoezinger, J. Catal. 167 (1997) 379.
[25] S.-I. Ito, C. Chibana, K. Nagashima, S. Kameoka, K. Tomishige, K. Kunimori, Appl. Catal. A 236 (2002) 113.
[26] R. Burch, M.I. Petch, Appl. Catal. A: Gen. 88 (1992) 39.
[27] I.C. Yates, C.N. Satterfield, Energy Fuels 5 (1991) 168.
[28] G.P. van der Laan, A.A.C.M. Beenackers, Appl. Catal. A: Gen. 193 (2000) 39.
[29] C.S. Kellner, A.T. Bell, J. Catal. 70 (1981) 418.
[30] C.G. Takoudis, Ind. Eng. Chem. Prod. Res. Dev. 23 (1984) 149.
[31] D.B. Dadyburjor, J. Catal. 82 (1983) 489.
[32] Y.I.P.N.V. Pavlenko, Theor. Exp. Chem. 33 (1997) 254.
[33] N.V.P.a.G.D.Z.A.I. Tripol'skii, Theor. Exp. Chem. 33 (1997) 165.
[34] S. Storsaeter, D. Chen, A. Holmen, Surf. Sci. 600 (2006) 2051.
[35] C. Mazzocchia, P. Gronchi, A. Kaddouri, E. Tempesti, L. Zanderighi, A. Kiennemann, J. Mol. Catal. A: Chem. 165 (2001) 219.
[36] B.H. Davis, Fuel Process. Technol. 71 (2001) 157.
[37] C.F. Huo, Y.W. Li, J.G. Wang, H.J. Jiao, J. Phys. Chem. C 112 (2008) 14108.
[38] M.A. Vannice, J. Catal. 37 (1975) 449.
[39] K.J. Williams, A.B. Boffa, M. Salmeron, A.T. Bell, G.A. Somorjai, Catal. Lett. 9 (1991) 415.
[40] G.A. Huff, C.N. Satterfield, Ind. Eng. Chem. Proc. Des. Develop. 23 (1984) 696.
[41] Y. Mori, T. Mori, T. Hattori, Y. Murakami, Appl. Catal. 66 (1990) 59.
[42] E. Shustorovich, A.T. Bell, J. Catal. 113 (1988) 341.
[43] Y. Mori, T. Mori, T. Hattori, Y. Murakami, Appl. Catal. 55 (1989) 225.
[44] Y. Kim, H.C. Peebles, J.M. White, Surf. Sci. 114 (1982) 363.
[45] L.J. Richter, B.A. Gurney, W. Ho, J. Chem. Phys. 86 (1987) 477.
[46] C. Egawa, S. Endo, H. Iwai, S. Oki, Surf. Sci. 474 (2001) 14.